

# Generation of a large scale atmospheric turbulence based on an improved fractal algorithm

ZHI SUN<sup>a,d\*</sup>, YING CHEN<sup>c</sup>, XIAOLIN QIN<sup>a</sup>, YONG FENG<sup>b</sup>

<sup>a</sup>Chengdu Institute of Computer Applications, Chinese Academy of Sciences, Chengdu, 610041, P.R. China

<sup>b</sup>Chongqing Key Laboratory of Automated Reasoning and Cognition, Chongqing Institute of Green and Intelligent Technology, Chinese Academy of Sciences, Chongqing, 400714, P.R. China

<sup>c</sup>Institute of Optics and Electronics, Chinese Academy of Sciences, Chengdu, 610209, P.R. China

<sup>d</sup>University of Chinese Academy of Sciences, Beijing, 100049, P.R. China

A rectangular phase screen transmission model is usually applied to the simulation of optical propagation processes in atmospheric turbulence. In this paper, we analyze the relationship between fractal Brownian motion and atmospheric turbulence firstly. Then based on the classical fractal algorithm, a new algorithm is proposed to generate a rectangular phase screen, which combines the random midpoint displacement (RMD) principle with the successive random additions (SRA) technique. It mainly contains three interpolation methods including square interpolation, trigonometric interpolation and diamond interpolation, respectively. Therefore we call the algorithm (S-T-D)RMD-SRA. We carry out the split-step method to propagate beam through atmospheric turbulence, which is simulated by a rectangular phase screens transmission model. Numerical simulations show that the new algorithm and traditional FFT-based algorithm on the statistical properties are almost consistent with the theoretical value. Furthermore, it has high performance in computation time and parallel efficiency.

(Received January 20, 2016; accepted August 3, 2016)

**Keywords:** Atmospheric Turbulence, Phase Screen, Fractal Interpolation, Beam Propagation, Parallel Computing

## 1. Introduction

In the development of wireless optical communication and ground-based telescope, laser radar, atmospheric turbulence has become one of the most important constraints [1,2]. An effective method in the research of atmospheric turbulence is the numerical simulation technique, which is based on a multi-phase screen transmission model. A turbulence phase screen is a two-dimensional array of random phase values on a grid of sample points and represents phase perturbations of a propagating wavefront through the atmosphere in accordance with Kolmogorov theory [3]. Turbulence-induced phenomena in optical propagation through the atmosphere were first studied by Tatarski for plane waves. There are several methods for generating turbulence phase screens, such as FFT-based method [4,5], Zernike polynomials method [6,7] and the covariance-based method [8]. The FFT-based algorithm is the most widely used phase screen generation algorithm, which is improved to some extent by the harmonic compensation method [9]. Generated by the Zernike polynomial algorithm, phase screen can consist with theoretical results in low frequency components. However, the high spatial frequency components of screens are insufficient. In the covariance-based method,

the simulation is very accurate, but the supported points of the screen are very small. In order to overcome these shortcomings, Lane [10] introduced the random midpoint displacement algorithm (RMD) [11] as an alternative way to generate phase screens based on the fractal characteristics of turbulence distorted wavefront. Considering the target linear velocity and transverse wind speed, a large scale rectangle turbulence screen is more appropriate in simulation system of the adaptive optics (AO) [12,13]. Due to move the multi-level rectangle screen, it is possible to save computer resource and improve the computational efficiency.

In this paper, we formalize the methods taken in a previous study and propose a new parallel algorithm based on the fractal theory. This algorithm combines the fractional Brownian motion (FBM) [14] principle with the successive random additions (SRA) [15] technique. And it mainly uses three interpolation methods, including trigonometric interpolation, square interpolation, and diamond interpolation. Simulation results indicate that the spatial phase structure function of a random phase screen generated by the new algorithm and FFT-based algorithm is almost consistent with the theoretical value. Referring to V. A. Banakh's experiments [16,17], we use the split-step method (SSM) to simulate the propagation of a Gaussian beam through the atmospheric turbulence.

And the scintillation index results show that both the new fractal algorithm and FFT-based algorithm have achieved good results. Furthermore, both in computation time and parallel efficiency the proposed algorithm has high performance.

### 2. Fractional Brownian motion characteristic of turbulence

The fractal theory originates from research on the length of Britain’s winding coastline. It has not been strictly defined thus far, but it is generally accepted that fractal has the following properties. Among the above characteristics, self-similarity is the most prominent, and fractal dimension provides a quantitative description approach. According to non-Kolmogorov, the phase structure function of phase screen is:

$$D_\beta(\rho, L) = C_\beta^2 \left(\frac{\rho}{r_{0,\beta}}\right)^{\beta-2} \tag{1}$$

where  $C_\beta^2$  represents the phase structure constant,  $L$  is the transmission distance. And  $r_{0,\beta}$  is the extended atmospheric coherence length,  $\beta$  represents the power-law exponent. Thus, the Hurst exponent  $H$  of FBS can be shown:

$$2H = \beta - 2 \tag{2}$$

In general, only if  $H=5/6$  and  $\beta=11/3$ ,  $D_\beta(\rho, L)$  can be used to describe the phase structure function of phase screen corresponding to Kolmogorov turbulence. The following sections we only discuss the situation of Kolmogorov turbulence for simplifying the computation process. For the Kolmogorov theory turbulence, structure function can be expressed as:

$$E < [\phi(r') - \phi(r)]^2 > = C_\phi^2 \left(\frac{|r - r'|}{r_0}\right)^{2H} \tag{3}$$

where  $E < >$  is the ensemble average,  $r_0$  is the atmospheric coherence length. And  $H$  represents the Hurst parameter which meets the following constraint equation:

$$F = E + 1 - H \tag{4}$$

which is called the fractal dimension between 0.5~1.  $E$  represents surface topology dimension. For plane,  $E = 2$ . As shown in Equation 3, set  $r = r - r'$  and  $H = 5/6$ . Then structure function is given by:

$$D_\phi(r) = 6.88(r / r_0)^{5/3} \tag{5}$$

From Equation 4 and 5, atmospheric turbulence can be described fractal Brownian motion which Hurst parameter is 5/6 and fractal dimension is 13/6. When all the edge point interpolations are finished, the remainder can be uniformly processed as inner point diamond

interpolations. Similar to square interpolation, the phase value of the interpolation point is the mean of four nearby points added with a random increment. Then, adjust the four interpolated corner points with independent random offsets, which share the same variance. Repeat the above steps until the grid is divided into the given n-level and generate a square phase screen, the size of which is  $(2^n + 1) \times (2^n + 1)$ .

### 3. Generation of a large scale phase screen based on (S-T-D)RMD-SRA

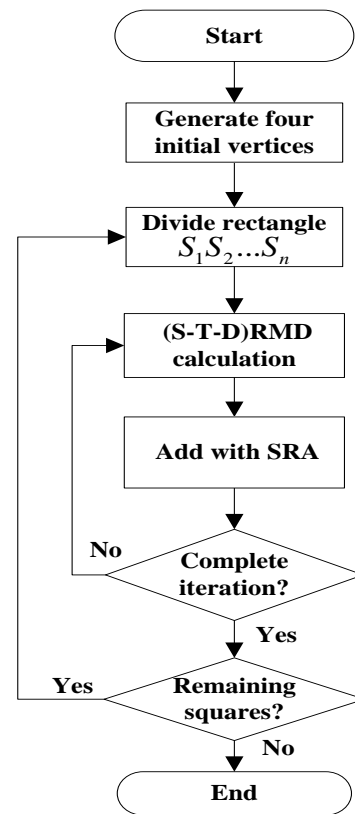


Fig. 1. General flow of the (S-T-D)RMD-SRA algorithm.

As shown in Equation 5, structure function can be used in the derivation algorithm to generate fractal basic formula. Since the grids generated by FBM are nonindependent, the computation amount of accurate fractal algorithms is very long considerably. The inter sample difference time series of FBM is called fractional Gaussian noise (FGN). Therefore, a simplified method called the successive random additions (SRA) is used to solve the problem. Considering the statistical characteristics of atmospheric turbulence, the key of the algorithm is dividing a rectangle into large amount of squares, then through fractal iteration process, combing a square-trigonometric-diamond(S-T-D)RMD algorithm with the SRA. During the interpolation process, interpolation points in edge positions are obtained by

trigonometric interpolation. Center points of squares are obtained by square interpolation. And other points are calculated by diamond interpolation. Fig. 1 shows the flow diagram of the algorithm.

### 3.1. Partition of a large scale rectangular phase screen into several squares

According to characteristics of the fractal iteration, we assume that the size of rectangle phase screen, length is  $l_1 (l_1 = 2^{N_1})$  and width is  $l_2 (l_2 = 2^{N_2})$ . Hence, the grid points of phase screen are  $(2^{N_1} + 1) \times (2^{N_2} + 1)$ . Firstly, it's necessary to calculate the four initial corner points. On account of the statistical properties and difference between rectangle's length and width, values of these initial points are defined as the linear combination of random variables by:

$$\begin{cases} \alpha = R_\alpha^a + R^b + R^c \\ \beta = R_\beta^a + R^b - R^c \\ \gamma = R_\gamma^a - R^b + R^c \\ \delta = R_\delta^a - R^b - R^c \end{cases} \quad (6)$$

where  $\alpha, \beta, \gamma, \delta$  represent the four corner of the rectangle, and  $R_\alpha^a, R_\beta^a, R_\gamma^a, R_\delta^a$  are Gaussian random variables, whose mean is zero and variance is  $\sigma_a^2$ .  $R^b, R^c$  are also Gaussian random variables, whose variance is  $\sigma_b^2$  and  $\sigma_c^2$  respectively. By Equation 5 and 6, we can derive the following equations:

$$\begin{cases} E < (\alpha - \beta)^2 > = 2\sigma_a^2 + 4\sigma_c^2 = 6.88(l_1 / r_0)^{5/3} \\ E < (\beta - \delta)^2 > = 2\sigma_a^2 + 4\sigma_b^2 = 6.88(l_2 / r_0)^{5/3} \\ E < (\beta - \gamma)^2 > = 2\sigma_a^2 + 4\sigma_b^2 + 4\sigma_c^2 \\ = 6.88(\sqrt{l_1^2 + l_2^2} / r_0)^{5/3} \end{cases} \quad (7)$$

By solving Equation 7, we can obtain  $\sigma_a^2, \sigma_b^2, \sigma_c^2$ . Then to take them into Equation 6, we can obtain four initial corner points. Next, it's necessary that the edges of rectangle phase screen are further subdivided by the RMD method, otherwise known as linear interpolation. For example, the midpoint between  $\alpha$  and  $\beta$  is  $P_1$ . So  $P_1$  can be expressed as  $P_1 = (\alpha + \beta) / 2 + \eta$ , where  $\eta$  is a Gaussian random variable with zero mean. According to Equation 5, we can deduce the general variance formula of linear interpolation. In the algorithm, the formula can be used in the following linear interpolation directly. It's only related to distance of endpoints ( $d$ ) and atmospheric coherence length ( $r_0$ ):

$$\Delta\sigma_{linear} = 0.447 \left(\frac{d}{r_0}\right)^{5/3} \quad (8)$$

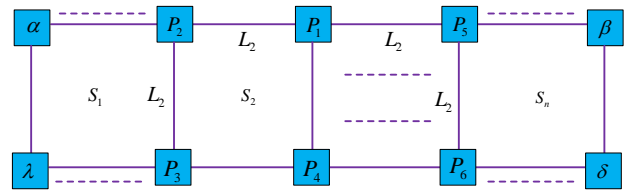


Fig. 2. Cropped a rectangle phase screen to multiple squares.

By this analogy, from  $\alpha$  to  $\beta$  and  $\gamma$  to  $\delta$ , we can calculate the midpoints by using the RMD method separately. As shown in Figure 2, through multiple iterations, rectangular phase screen can be divided into  $n (n = N_1 / N_2)$  square with side length  $l_2$ .

### 3.2. (S-T-D)RMD-SRA Fractal Algorithm

In many respects the non-stationary artifacts of RMD are similar to the staircase effect of aliased raster display lines including fractal phase screen. With RMD only, once determined, the value at a point remains fixed. At each stage only half of the points are determined more accurately. In term of the Nyquist sampling theorem, to approximate  $N$  real points requires  $N/2$  complex frequencies or  $N/2$  sine and cosine components. The process of adding randomness to all points at each stage of a recursive subdivision process is successive random addition (SRA).

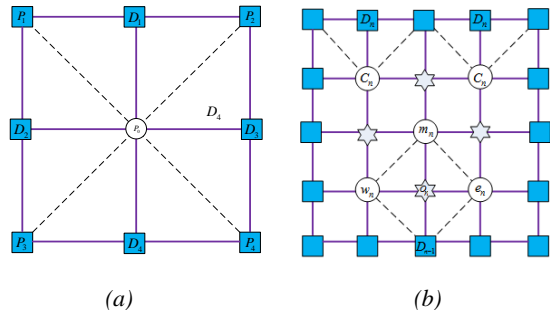


Fig. 3. Schematic diagram of (S-T-D)RMD-SRA. (a) Square interpolation. (b) Trigonometric and diamond interpolation.

This enhancement reduces many of the visible artifacts of RMD and the generation still requires only order  $N$  operations to generate  $N$  points. In order to better illustrate the principles of (S-T-D)RMD-SRA fractal algorithm, we take a square generation as an example. The basic steps are made up of four interpolations:

1. Square interpolation. As shown in Fig. 3(a), the center point is interpolated in the each recursive small square, and the value of each interpolation point is the mean of four nearby corner points added with a random Gaussian variable:

$$P_0^i = (P_1^i + P_2^i + P_3^i + P_4^i) / 4 + \varepsilon_s^i \quad (9)$$

where  $\varepsilon_s^i$  is the  $i$ th square interpolation increment

with variance  $\Delta \varepsilon_s^i$ . In order to obtain  $\Delta \varepsilon_s^i$ , there is a easily proven fact for any three random variables: It can be developed from values of the mean square difference between values of  $x$  and  $z$ , using the easily proven fact<sup>[18]</sup> that for any three random variables, say  $\kappa, \mu, \rho$  having zero mean and equal variances.

$$\langle (\kappa - \mu)(\rho - \mu) \rangle = \frac{1}{2} \{ (\kappa - \mu)^2 + (\rho - \mu)^2 - (\kappa - \rho)^2 \} \quad (10)$$

One approach to deal with the non-stationarity of RMD technique with SRA. Therefore, each interpolation it's necessary to adjust the four corner points by SRA, which share the same  $\Delta \varepsilon_s^i$ :

$$\begin{aligned} P_1^i &= P_1^{i-1} + \Delta \varepsilon_s^i & P_2^i &= P_2^{i-1} + \Delta \varepsilon_s^i \\ P_3^i &= P_3^{i-1} + \Delta \varepsilon_s^i & P_4^i &= P_4^{i-1} + \Delta \varepsilon_s^i \end{aligned} \quad (11)$$

In the proposed fractal algorithm, we can use the Equation 12 in the following square interpolation directly. It's only related to side length of squares and atmospheric coherence length:

$$\Delta \varepsilon_s^i = 0.609 \left( \frac{l}{r_0} \right)^{5/3} \quad (12)$$

2. Trigonometric interpolation. Figure 3(a) shows the process. Edge points like  $D_1, D_2, D_3, D_4$  are interpolated in the vertex of each recursive small trigonometric. It's an important improvement compared with the linear interpolation, which introduces more structure correlations between points on the phase screen. The value of  $D_1$  is given by:

$$D_1^i = q^i (P_1^i + P_2^i) + (1 - 2q^i) P_0^i + \varepsilon_i^i \quad (13)$$

where  $q^i$  set to 1/2 or 1/3. It's the  $i$ th weighting coefficient.  $\varepsilon_i^i$  is the  $i$ th edge point trigonometric interpolation increment. The variance  $\Delta \varepsilon_t^i$  is given by:

$$\begin{cases} \Delta \varepsilon_t^i = 0.209 \left( \frac{l}{r_0} \right)^{5/3} & \text{if } q^i = 1/3 \\ \Delta \varepsilon_t^i = 0.447 \left( \frac{l}{r_0} \right)^{5/3} & \text{if } q^i = 1/2 \end{cases} \quad (14)$$

3. Diamond interpolation. As shown in Fig. 3(b), point like  $o_n$  is at the special position, which belongs to inner square but not center point. Similar to square interpolation, we can obtain its value by diamond interpolation:

$$o_n^i = (m_n^i + w_n^i + D_{n-1}^i + e_n^i) / 4 + \varepsilon_d^i \quad (15)$$

where  $\varepsilon_d^i$  is the  $i$ th edge point diamond interpolation increment. The variance is given by:

$$\Delta \varepsilon_d^i = 0.342 \left( \frac{l}{r_0} \right)^{5/3} \quad (16)$$

where  $l$  represents side length of squares and  $r_0$  is atmospheric coherence length. Similarly, we use the SRA method to adjust the four interpolated corner points with independent random offsets, which share the same variance.

Parallel iteration  $S_1 \rightarrow S_n$ , until all squares are divided into the given  $N_2$ -level and obtain a very large scale rectangle phase screen, the total grid points of phase screen are  $(2^{N_1} + 1) \times (2^{N_2} + 1)$ .

## 4. Simulation results and analysis

In order to provide a complete evaluation of the improved algorithm, we generate a rectangular phase screen utilizing the algorithm introduced last section. Firstly we will compare spatial statistics of the generated rectangular with theoretical values. The accuracy and efficiency of the above-mentioned algorithm can be tested and evaluated. Then for purpose of obtaining results of scintillation index, we use the split-step method to propagate beam through atmospheric turbulence, which is simulated by a rectangular phase screens transmission model. Finally we carry out the parallel computing of experiments and test the parallel speedup of the algorithm by compared the average time of generating a single random phase screen of the above-mentioned algorithm. We take two sets of experiment platforms for testing performance comprehensive. Table 1 shows the hardware and software configuration of experimental computers.

Table 1. Hardware and software configuration of experimental computers.

	OS	CPU	Memory	Software
Computer 1	Win7	Intel i72600 (3.4 GHz)	4GB	Matlab 2014a
Computer 2	Fedora20	AMD X4 955(3.2GHz)	4GB	Matlab 2014a

### 4.1. Comparison of the spatial characteristics

The spatial phase structure function curves of the random phase screen generated by the FFT-based algorithm and (S-T-D)RMD-SRA fractal algorithm are shown in Fig. 4, in which the Fig. 4(a) and 4(c) is presented by linear coordinate and the Figure 4(b) and 4(d) is presented by logarithmic coordinate. By using FFT-based algorithm, we firstly generate a square phase screen whose grid points are  $256 \times 256$ . And then generate a  $256 \times 8192$  rectangular screen by using the algorithm proposed in this paper. The grid points of selected rectangular part are also  $256 \times 256$ . The simulated results are the ensemble average of 10,000 times from such the  $256 \times 256$  part and compared with

the theoretical one. Some parameters which are used to generate a rectangular random phase screen are as follows. The telescope aperture is 1.20m, the Gaussian beam radius is 42.42cm, the coordinate transformation factor is 75679.24m (divergent coordinate system), sampling interval is 0.001m, and atmospheric coherence length is 0.3m. Wind speed is 2m/s.

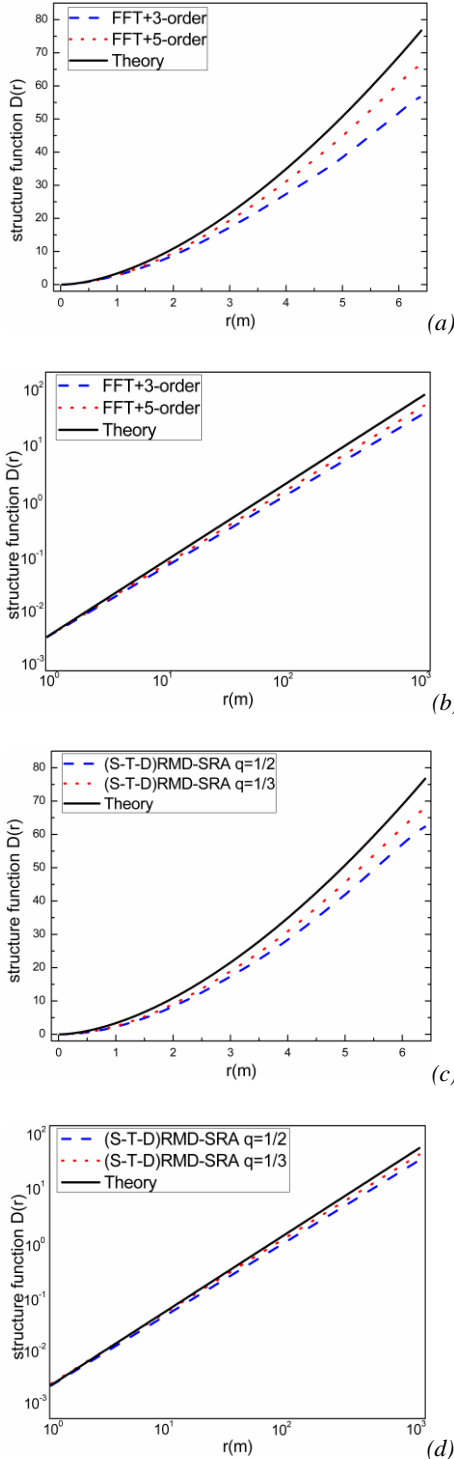


Fig. 4. Comparison of the phase screens spatial structure functions; (a), (b) FFT-based algorithm structure function; (c), (d) (S-T-D)RMD-SRA algorithm structure function.

As can be seen in Fig. 4(a) and 4(b), the spatial structure function of random phase screen generated by the FFT algorithm is close to the theoretical values, especially existing high-order harmonic compensation. While in Fig. 4(c) and 4(d), the curve generated by the (S-T-D)RMD-SRA algorithm is also close to the theoretical values. In addition, when the edge points takes the trigonometric interpolation (weight coefficient  $q=1/3$ ), the effect of the algorithm is better than take the linear interpolation (weight coefficient  $q=1/2$ ). In conclusion, the structure function obtained from the present algorithm agree well with the theoretical, as well as traditional FFT-based algorithm, especially weight coefficient  $q$  is  $1/3$ .

#### 4.2. Simulation results of beam propagation through atmospheric turbulence

In addition to the comparison of the spatial statistics, a numerical simulation was performed to check the validity of this algorithm, in which we use the split-step method(SSM)<sup>[19]</sup> to simulate the propagation of a Gaussian beam through a set of random phase screens generated by the algorithm discussed in the previous section. As statistical indicators, the scintillation index  $\sigma_1^2(x)$  is defined as<sup>[20]</sup>:

$$\sigma_1^2(x) = \frac{\langle I(x,0)^2 \rangle}{\langle I(x,0) \rangle^2} - 1 \quad (17)$$

where  $I$  is the received light intensity and  $\langle \rangle$  represents ensemble averaging,  $\sigma_1^2(x)$  can be obtained through transmitting random phase screens.

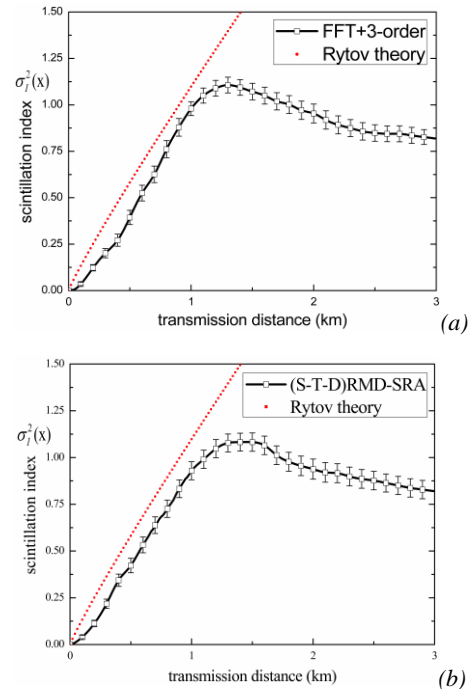


Fig. 5. Scintillation index with error bar. (a)FFT+3-order algorithm. (b)(S-T-D)RMD-SRA algorithm.

The parameters used in our simulations are setting as follow: the wavelength is  $1.315\mu\text{m}$ . Inner scale  $l_0$  is  $1.5\text{mm}$  and outer scale  $L_0$  is  $0.384\text{m}$ , representing a grid distance and screen width respectively. The beam path has been divided in 10 consecutive phase screens, each of them covering a propagation distance  $\Delta z=50\text{m}$ . Finally, the overall propagation distance is  $3\text{km}$ . The value taken for the turbulence strength constant  $C_n^2$  is  $5 \times 10^{-14} \text{m}^{-2/3}$ . The size of screens  $N_x \times N_y$  is  $256 \times 8192$  pixels. Then we can calculate  $r_0 = 0.148\text{m}$ . In order to obtain the scintillation index accurately, we have performed a series of 1000 beam propagation simulations by using the SSM. As shown in Fig. 5, the results for plane wave optical propagation in a turbulence atmosphere exhibiting normalization Kolmogorov scintillation index are computed. Simulation results of FFT+3-order algorithm and (S-T-D)RMD-SRA algorithm are shown in Fig. 5(a) and 5(b), respectively. The theoretical curve obtained by Rytov approximation is defined as  $\sigma_1 = (1.23C_n^2 k_0^{7/6} z^{11/6})^{1/2}$ . The corresponding error bars of the scintillation index generated by two algorithms are shown in Fig. 5.

We can see in Fig. 5, with the transmission distance increasing, the scintillation index curves made with the (S-T-D)RMD-SRA algorithm and other algorithms increase first quickly and then show the saturation trend obviously. This effect is important in the weak turbulence

regime. In the weak fluctuation situation, all two numerical simulation results are approximately identical to the theoretical curves of Rytov theory. The reason of such situation can be explained by the fact that in both cases the Rytov theory itself under weak fluctuation situation is not consummate. Hence, comprehensive results for the statistical quantities are not yet available. In this respect, the beam propagation through turbulent atmosphere should provide useful contributions to a better understanding of phase screens. In summary, the performance of two algorithms in terms of the scintillation index is similarly under the weak fluctuation situations.

### 4.3. Complexity and efficiency analysis

The algorithm complexity can be reflected by the average time of generating a single random phase screen. The simulated results are the ensemble average of 10,000 times by using two difference platforms. Fig. 6(a) and Fig. 6(c) shows the relationship between average generating time and phase screen size based on the FFT-based algorithm and (S-T-D) RMD-SRA fractal algorithm, respectively. It can be seen that, in terms of the average generating time, the FFT-based algorithm without harmonic compensation and (S-TD)RMD-SRA fractal algorithm are superior to remaining algorithms.

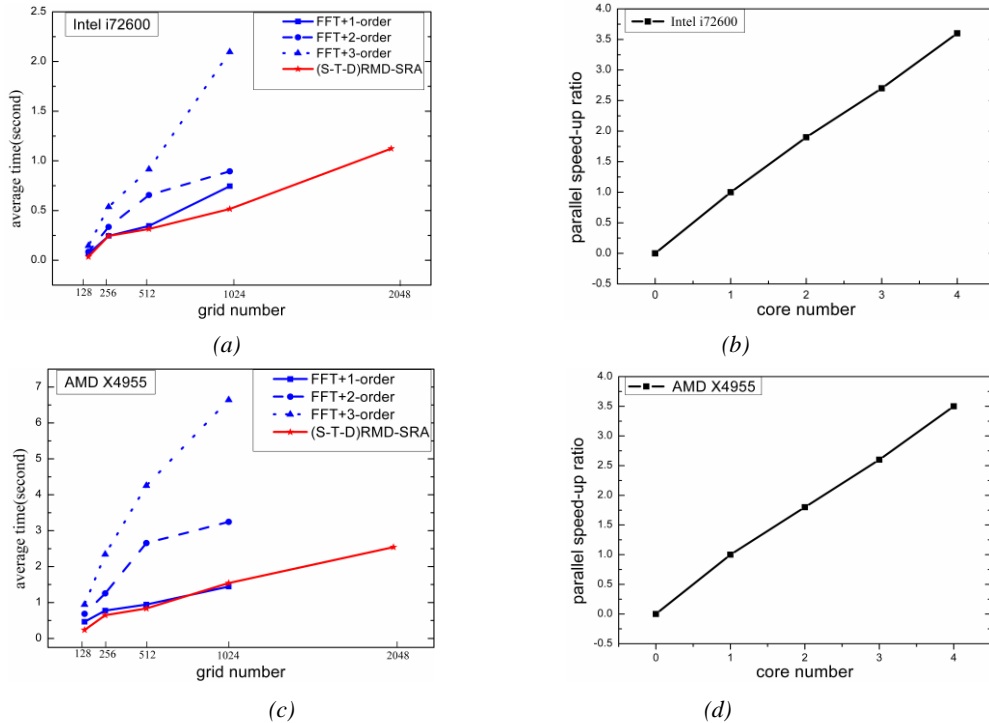


Fig. 6. Simulation time-consuming and parallel speed-up ratio of two platforms; (a),(b) Time-consuming and parallel speed-up ratio (Computer1). (c),(d) Time-consuming and parallel speed-up ratio(Computer2).

Furthermore, the algorithm proposed in this paper can be executed in parallel mode. As shown in Fig. 6(b) and 6(d), with increasing numbers of processing cores, speed-up ratio of both two platforms have different

degrees of improvement. When using two processing cores, the speed-up ratio of the algorithm is about 1.8 and 1.9. When using four processing cores, the ratio is about 3.7 and 3.6. For generating a  $P \times Q$  grid points, the

computational complexity of the present algorithm is  $\Theta(PQ)$ , while that of FFT-based algorithm is  $\Theta(\max(P^2 \log_2 P, Q^2 \log_2 Q))$  without harmonic compensation and  $\Theta(\max(P^2 \log_2 P + 27N, Q^2 \log_2 Q + 27Q))$  with 3-order harmonic compensation.

## 5. Conclusion

In order to simulate the optical transmission process in atmospheric, rectangle turbulence phase screen with large scale is used to represent the phase perturbations induced by a turbulent media in numerical simulation of light propagation through the atmosphere. According to the statistical characteristics of atmospheric turbulence, an improved algorithm called (S-T-D)RMD-SRA is proposed to generate a very large scale rectangle phase screen. Then, we analyze the reliability of this algorithm from precision and efficiency.

In terms of algorithm efficiency, the (S-T-D)RMD-SRA fractal algorithm is very efficient. We compare the spatial phase structure function as edge points taken the trigonometric interpolation ( $q=1/3$ ) and linear interpolation ( $q=1/2$ ). Experimental results indicate that the trigonometric interpolation ( $q=1/3$ ) has better performance. In addition, scintillation index results show the performance of the proposed algorithm is similar to traditional FFT-based algorithm. Therefore, it might be particularly useful for propagation problems involving a large space as with multiple beams such as phased arrays or where a beacon projector is spatially separated from the receiving aperture. It can be concluded that the improved fractal algorithm has high performance, comprehensively considering precision and efficiency. Hence, the phase screen generated by the algorithm can be used to simulate a large scale rectangular atmospheric turbulence.

## General remarks

The paper proposed generation method of a large scale rectangular phase screen the (S-T-D)RMD-SRA fractal algorithm. The improved algorithm has high performance, comprehensively considering precision and efficiency. Methodology of investigation and study is of vital importance. Other research forms are demonstrated in Ref [21, 22].

## Acknowledgements

This work is partially supported by China 973 Project (Grant No.NKBRPC-2011CB302402), National Natural Science Foundation of China (Grant Nos. 61402537,91118001), the West Light Foundation of the Chinese Academy of Sciences from China and the Open Project of Chongqing Key Laboratory of Automated Reasoning and Cognition from China (Grant No.CARC2014004).

## References

- [1] Hanling Wu, Haixing Yan, Xinyang Li, Shushan Li, Optics Express **17**(17), 14649 (2009).
- [2] Huili Zhai, Bulan Wang, Jiankun Zhang, Anhong Dang, Applied Optics **54**(13), 4023 (2015).
- [3] D. L. Fried, Journal of the Optical Society of America, **55**(11), 1427 (1965).
- [4] B. L. McGlamery, Journal of the Optical Society of America **57**(3), 293 (1967).
- [5] J. M. Martin, Stanley M. Flatte, Applied Optics **27**(11), 2111 (1988).
- [6] J. Robert Noll, Journal of the Optical Society of America **66**(3), 207 (1976).
- [7] A. Nicolas Roddier, Optical Engineering **29**(10), 1174 (1990).
- [8] M. Cressida Harding, A. Rachel Johnston, G. Richard Lane, Applied Optics **38**(11), 2161 (1999).
- [9] J. A. Jr. Fleck, J. R. Morris, M.D. Feit, Applied physics **10**(2), 129 (1976).
- [10] R. G. Lane, A. Glindemann, J. C. Dainty, Waves in Random Media **2**(3), 209 (1992).
- [11] Ilkka Norros, Petteri Mannersalo, L. Jonathan Wang, Advances in Performance Analysis **2**(1), 77 (1999).
- [12] Peng Jia, Dongmei Cai, Dong Wang, Alastair Basden, Monthly Notices of the Royal Astronomical Society **447**(4), 3467 (2015).
- [13] Ying Chen, Yong Feng, Journal of Computational and Theoretical Nanoscience **11**(6), 1433 (2014).
- [14] C. Schwartz, G. Baum, E. N. Ribak, Journal of the Optical Society of America A, Optics and Image Science **11**(1), 444 (1994).
- [15] R. Donald McGaughey, J. M. George Aitken, Physica A: Statistical Mechanics and its Applications **277**(12), 25 (2000).
- [16] V. A. Banakh, I. N. Smalikho, A. V. Falits, Atmospheric and oceanic optics, **25**(2), 106 (2012).
- [17] V. A. Banakh, I. N. Smalikho, Optics express **22**(19), 22285 (2014).
- [18] L. David Fried, Tim Clark, Journal of the Optical Society of America A, Optics and Image Science **25**(2), 463 (2008).
- [19] M. Z. M. Jenu, D. H. O. Bebbington, In Antennas and Propagation, 1993, Eighth International Conference, p. 817, IET, 1993.
- [20] L. C. Andrews, M. A. Al-Habash, C. Y. Hopen, R. L. Phillips, Waves in Random Media, **11**(3), 271 (2001).
- [21] E. L. Pankratov, E. A. Bulaeva, Reviews in Theoretical Science **1**(1), 58 (2013).
- [22] Michael Lipkind, Reviews in Theoretical Science **1**(2), 145 (2013).

\*Corresponding author: china.sunzhi@gmail.com